Evidence for quantized electronic level structure for 100–1300 electrons in metal-atomic clusters

John L. Persson, Robert L. Whetten
Departments of Chemistry and Physics, and Solid State Science Center, University of California, Los Angeles, CA 90024, USA

Hai-Ping Cheng and R. Stephen Berry
Department of Chemistry and The James Franck Institute, University of Chicago, 5735 South Ellis Avenue, Chicago, IL 60637, USA

Received 29 May 1991; in final form 26 August 1991

Photoionization mass spectrometry experiments on cold and warm beams of Al_N and In_N clusters reveal large, N-specific discontinuities in their cohesive and ionization properties. These can be interpreted in terms of bunching of electron levels – large-shell structure – through agreement with calculations based on the spherical-jellium approximation. Specific deviations found for intermediate-size Al_N, and differences between aluminum and indium, are attributed to the perturbation by the ionic lattice of the spherical jellium orbitals.

1. Introduction

In an early picture [1] of small metal particles, presumed irregularities in particle shape or environment cause the independent-electron energy levels to be nondegenerate and quasi-uniformly distributed, giving rise to a monotonic increasing density of states. Theoretical models derived within the corresponding random matrix formalism provided predictions for a quarter-century's experiments on the quantum size effects [#1]. In 1984, however, an entirely opposite starting point was used to explain the abundance anomalies ("magic numbers") found in alkali metal cluster beams. Knight et al. [3] showed that these are predicted by a spherical shell model [3], in which the conduction electrons form a quantized Fermi gas confined to a spherically symmetric potential well. An N-atom cluster is assigned $n_e = ZN$ conduction electrons, where Z is the atomic valency. The assumption of spherical symmetry dictates that the electrons fill the set of delocalized orbitals nl in the following sequence:

$$1s^2 1p^6 1d^{10} 2s^2 1f^{14} 2p^6 1g^{18} 1d^{10} 3s^2 1h^{22} 2f^{14} 3p^6 1i^{26} \ldots .$$

Here, the notation is $nl^{2(2l+1)}$, with n the radial quantum number, l the angular momentum quantum number and $2(2l+1)$ the degeneracy of the orbital. The level ordering is found to depend only weakly on the particular details of the radial shape of the potential. Qualitatively, trends in properties computed from a spherical-jellium background model (SJBM) [4] agree with experimental results for many clusters particularly of alkali metals [5], and the omitted important effects, such as ellipsoidal distortions and the ionic lattice, can be incorporated perturbatively into the model [6]. Recent experiments support this basic picture up to at least $n_e = 200$ electrons [7]. For some metals the jellium model fails to predict certain physical properties, e.g. the "dip" on the ionization curve of Al clusters at $N = 55$, which is not due to the gap between two jellium energy levels [8,9]. These have been accounted for by more sophisticated methods used to investigated the effect of the crystal-field splitting and the structure of the clusters [10].

Ordinarily, even the high degeneracies of spherical symmetry would fail to prevent the mean gap between energy levels from decreasing rapidly with in-

[#1] For a recent review, see ref. [2].

creasing cluster size, so that one might expect that even just a little smoothing would produce a monotonic electronic density of states (DOS) for large enough clusters [6]. However, model calculations have long indicated that the spacings need not fluctuate randomly and the DOS need not be monotonic [11,12]. Instead one finds a remarkable modulation of the energy level pattern, with the levels grouped together into large sets of electronic shells, leaving gaps between the shells (fig. 1) [13]. (Such eigenvalue density fluctuations were first studied in ideal boundary-value problems [11] and proposed to occur in heavier nuclei (where the term "super shells" originated, originally proposed as "gross shells") [12].) This modulation, periodic in square-root of the energy (momentum), is in turn modulated by a longer-wavelength oscillation, with the term "super shells" being used to describe this oscillation [11,12]. (The size-scalings of the mean level spacings (δ) are then: in the Kubo theory [1] (all energy levels) $\delta \sim E_F N^{-1}$, in the spherical shell model (between spherical shell levels) as $E_F N^{-1/3}$ and in the supershell picture (between shells) as $E_F N^{-1/6}$.)

Evidence for this type of grouping of levels into shells, with the shell size increasing with increasing energy, has very recently been observed in the stability and ionization-energy patterns of monovalent ($Z=1$) metal clusters Na_N and Cs_NO, with the results matching the spherical predictions $n_e = 1500$ electrons [14,15]. For Na_N larger than 1500 atoms [16], and also Mg_N clusters [17], a different effect – close packing of atoms into structural shells – gives rise to discontinuities each time a close-packed shell of atoms is completed, an effect that naturally is outside of the domain of the spherical-jellium picture. Until now there has been no experimental evidence reported for clusters to exhibit supershells with longer

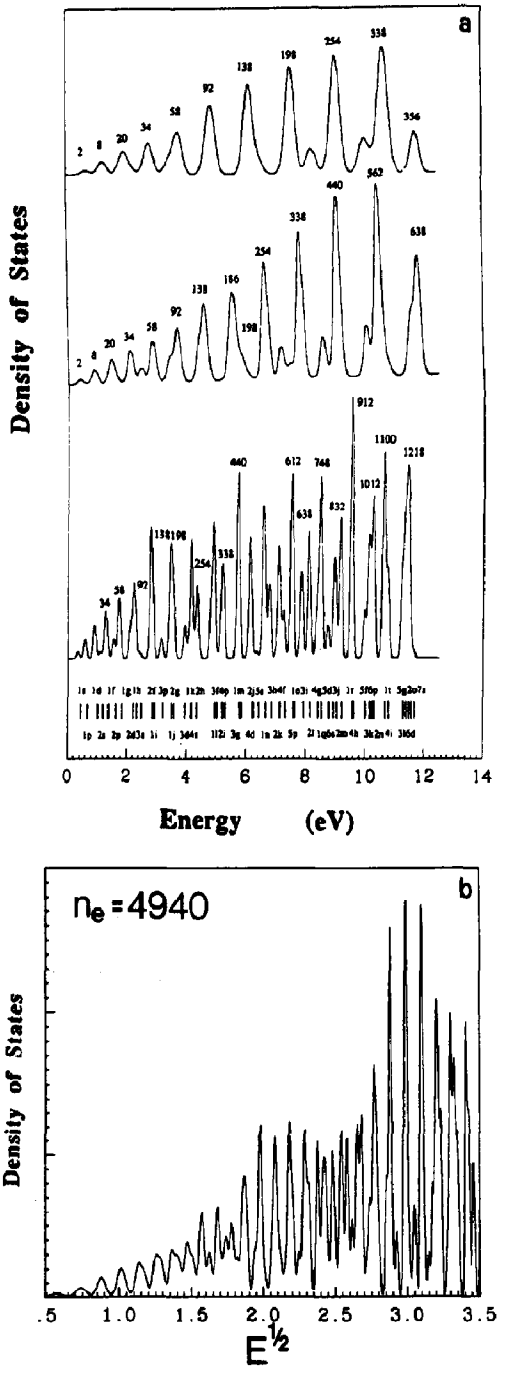

Fig. 1. Independent-electron state densities computed using the spherical-jellium background model, as solved self-consistently in the local-density approximation, for the size parameter appropriate to the metal aluminum, specifically $r_{Al} = 2.98\, a_0$. (Note the nearly constant Fermi energy, $E_F \approx 12$ eV, for Al clusters.) (a) The energy levels indicated at the bottom are annotated by their (n, l) quantum numbers. The curves calculated for $n_e = 1218$, 638 and 356 electrons, from bottom upward, have respective smoothing widths of 0.05, 0.1 and 0.15 eV. Integers above large peaks are the cumulative number of electrons needed precisely to fill that peak. (b) As in (a), but now plotted versus $E^{1/2}$ (~momentum) for $n_e = 4940$, to illustrate the super shell beat pattern in the density oscillations, as in the infinite-well potential [9]. For reference, the peaks concluding at 1.5 and 2.35 $(eV)^{1/2}$ have cumulative electron numbers of 220 and 1218, respectively.

wavelength modulation [11,12].

Here we report observations on the trivalent ($Z=3$) metal clusters Al_N (to $N=430$ atoms, or $n_e=1300$ electrons) and In_N (to $N=120$, $n_e=360$). Photoionization experiments on beams of these clusters reveal large, N-specific irregularities in electronic and cohesive properties, which are interpreted, through comparison to spherical-jellium model predictions, as evidence for a modulated electronic density of states, with the levels grouped in shells. For aluminum clusters, the observed pattern agrees well with the calculations from the spherical model only for large clusters, $N>250$. We attribute this to the strength of the perturbation from the trivalent ionic lattice in small clusters [8].

2. Experimental methods

The experimental setup is basically the same as that described previously [8]. The laser-ablation jet source, with its nozzle in the shape of a long, narrow slit, produces large clusters through long residence-times and number of collisions. The clusters are ionized close to the source (15 cm), and subsequently mass analyzed in a Wiley–McLaren TOFMS [18], oriented collinear with the cluster beam to increase its mass range (fig. 2).

Photoionization mass spectra of Al_N and In_N, taken near or above ionization threshold, can reveal the electronic structure in two different ways. Near threshold, the closing of electronic shells of large clusters can well be associated with a steplike *increase* in photoionization cross section after the shell closing, as a new higher energy shell is opened. Well above threshold, cluster stability differences are manifested in the relative abundances, with steplike *decreases* in the mass spectra after a shell closing. These are each familiar concepts in cluster beam methodology [5,7]. Finally, as a means of discriminating between the different effects, the cluster source can be cooled to liquid nitrogen temperatures, lowering the condensation temperature at which the clusters are formed to 110 K, freezing in the kinetically determined size distribution and thereby effectively eliminating abundance variations arising from stability differences.

3. Experimental results

Examples of threshold-region photoionization mass spectra of Al_N and In_N clusters are shown in fig. 3. The step-like increases at $N=46$–47 and 66–67 are associated with calculations showing gaps after the completion of shells (fig. 1) at $n_e=138$ and 198 electrons, and with significant decreases in the ionization potential accompanying the shell openings [8]. The latter, 60-electron level bunch (fig. 1), has, as its highest filled angular momentum levels the con-

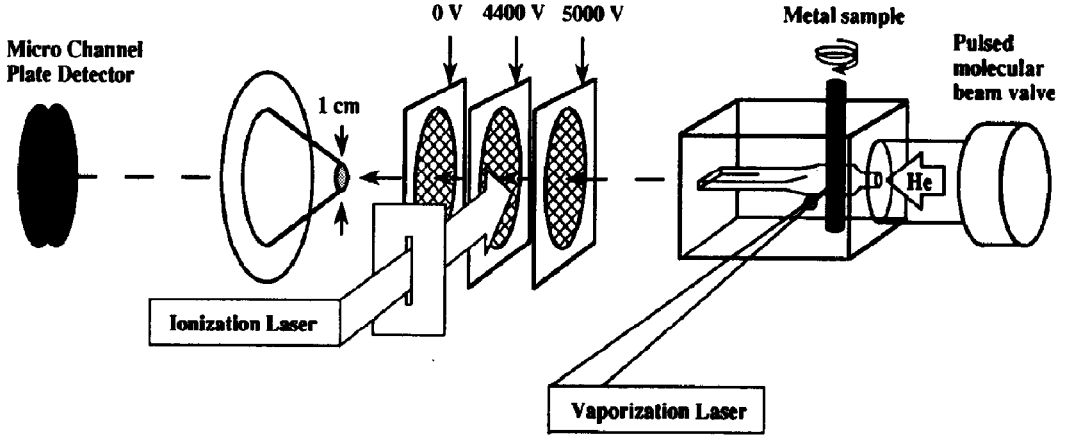

Fig. 2. Schematic diagram of the experimental apparatus (not to scale).

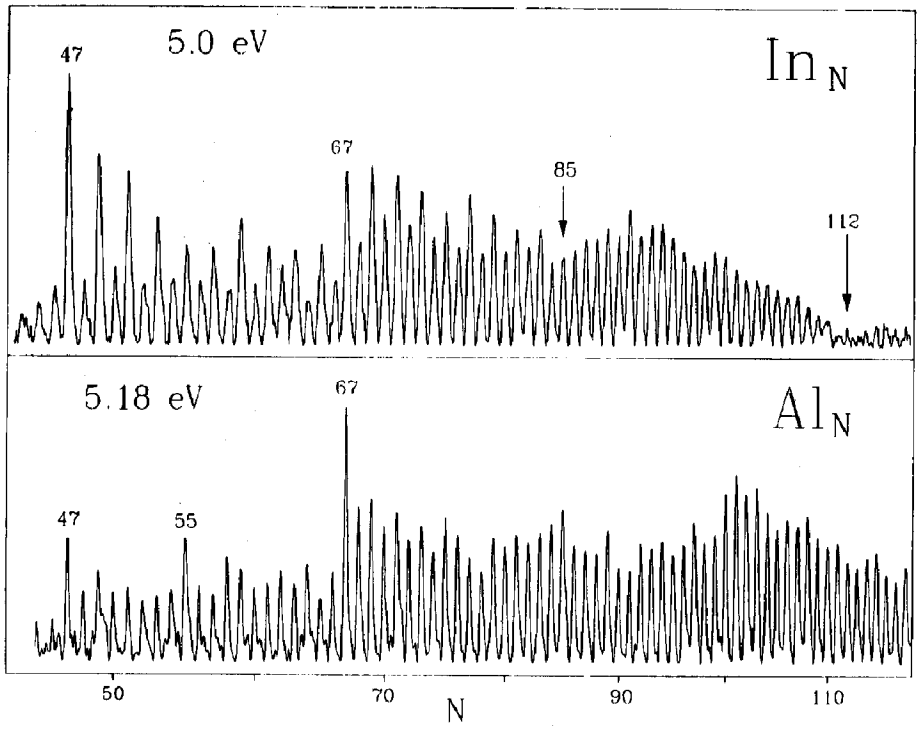

Fig. 3. Photoionization mass spectra of aluminum (at 5.18 eV) and indium clusters (at 5.00 eV), in the $N=40$–120 range, as observed near the ionization threshold. The increases at $N=47$, 67, 85 and 113 atoms correspond to the first clusters after the predicted shell closings at $n_e=138$, 198, 254, and 338 electrons.

figuration ($1j^{30}2g^{18}3d^{10}4s^2$). The absence of other major features in this region, particularly for In, indicate dominance of electronic shell closure on the electronic structure of clusters in this size-range. In the mass spectrum of In clusters taken at 5.0 eV, two other features appear at larger N: (i) At $N=85$ the odd–even alternations disappear and a slight but reproducible inflection occurs, and (ii) a major minimum occurs in the $N=109$–112 range, with recovery at 113–114. Each of these are manifestations of further shell closings, and correspond well to the next shells expected to fill at $n_e=254$ and 338 electrons (fig. 1). No other discontinuities are observed for Al_N up to $N=140$ atoms, with the exception of a weak ledge at $N=100$–101 atoms.

In fig. 4, two mass spectra of Al_N at a photon energy of 6.4 eV are compared, for source condensation temperatures $T=290$ K and $T=110$ K. Features due to photoionization cross section are independent of source temperature, and are thus present in both spectra. Shell closings at 68 electrons (22–23 atoms), 138 electrons (46–47 atoms) and 198 electrons (66–67 atoms) are apparent through the decreases in cross section at these cluster sizes, even well above threshold. A few of the smaller clusters, $N<14$, are absent in both spectra because of their high ionization potentials [8]. For $N>140$ atoms, a sequence of weak local abundance maxima is observed, identified as stability related variations from their disappearance at 110 K.

When the photon energy is lowered to 5.0 eV, still above threshold for $N>140$, the same abundance ledges are observed, showing that these features are independent of the ionizing laser frequency (fig. 5). (The corresponding distribution obtained from the cold source (not shown) is very smooth.) The gradual increase before each maximum and the following steep drop is typical of electronic shell structure as revealed through preferential evaporation, in the source, of clusters just larger than the closed-shell

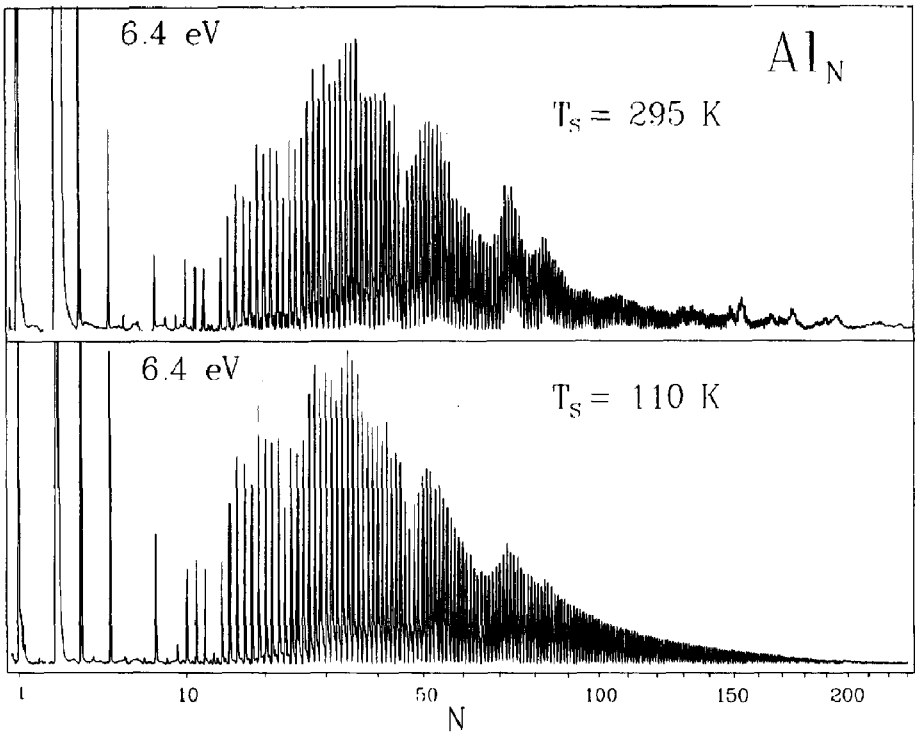

Fig. 4. Photoionization mass spectra of Al_N at two source temperatures, 295 and 110 K, showing the temperature dependence of the abundance fluctuations present for $N > 140$ atoms in the 295 K spectra.

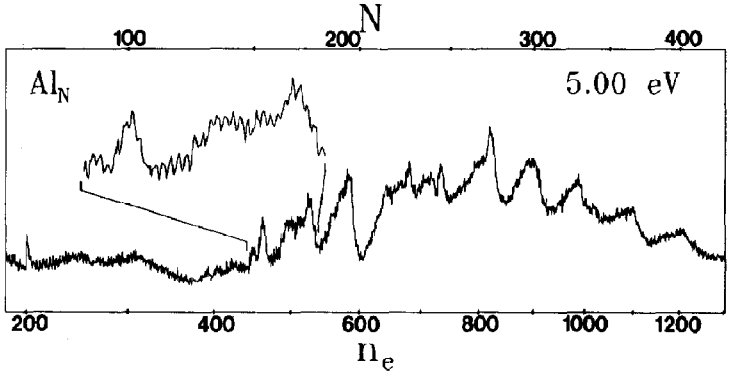

Fig. 5. Time-of-flight mass spectrum of larger aluminum clusters (N=60–435) produced in the 300 K source, and photoionized above threshold at 5.00 eV. The inset shows individual mass peaks in the N=149–180 region.

clusters. Individual mass peaks are resolved out to N=300 atoms (see inset in fig. 5), but beyond N=300, only the average variation is observed. Following ref. [12], the logarithmic derivative of the peak intensities I_N with respect to the number of electrons n_e is computed, in order to extract the electron-number n_e^* at each shell closing: $d(\ln I_N)/dn_e$. This quantity is shown in the top part of fig. 6, where each peak corresponds to a steep drop in fig. 5.

The n_e^* values found in this way are collected in table 1, where they are compared with the computed shell-filling numbers, indexed by the maximum an-

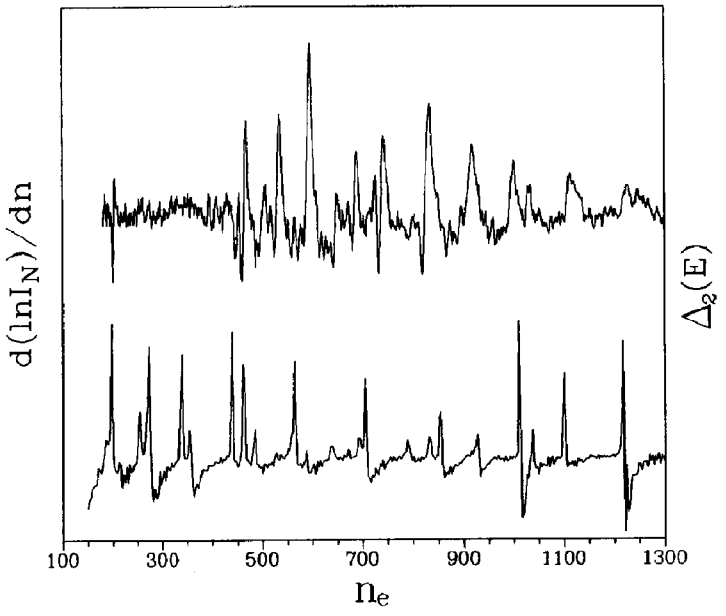

Fig. 6. Upper curve: logarithmic derivative, $d(\ln I_N)/dn_e$ versus n_e, of the Al_N abundances from fig. 5. Lower curve: the second difference in the total electronic energies of Al_N, computed from the spherical-jellium background model, showing the predicted abundance anomalies.

Table 1
Predicted and observed shell-filling numbers [a], n_e^*

l_{max}	Predicted	Al	In
6	138	138	138
		164	
7	198	198	198
8	254		252
9	338	336	
10	440, 462	438 [b], 468±6	
	556	534±6	
11	588 [a]	594±6	
12	694	688±6	
13	760	742±6	
	832	832±10	
14	926	918±10	
	1012	1000±10	
15	1100	1112±10	
	1218	1224±10	

[a] Predicted electron shell-filling numbers (n_e^* from spherical-jellium calculations (fig. 6), indexed by the angular momentum quantum number l_{max}. Experimental values correspond to ionization cross section increases (for $n_e < 400$) or to abundance ledges ($n_e > 400$); in the latter case they are assigned from the logarithmic derivative shown in fig. 6.

[b] Predicted shell-closing with a gap sensitive to the reference-size used.

[c] A positive-going ledge, possibly indicating a major ionization potential increase.

gular momentum quantum number l_{max}. The agreement becomes increasingly good at larger cluster sizes ($N > 250$ atoms), and the five major high-N features are in excellent correspondence with the calculated shell closings. In the size range $140 < N < 250$ atoms, only about half the observed features match the calculations. The most likely explanation is the perturbation caused by the ionic lattice. As explained in our earlier work [8], the ionic cores of $+3e$ charge constitute a non-negligible perturbation. The improved agreement with the spherical model with increasing N is expected from the lessened influence, particularly on low-l orbitals, of the ionic lattice in larger clusters. Detailed consideration of the discrepancies with the spherical model may allow a better determination of the correct effective potential for electrons in Al_N particles. Finally, the absence of discontinuities in the range $100 < N < 140$ atoms may correspond to the first minimum in the super shell modulation (fig. 1b), but it would be premature to make the assignment of the oscillation based on only one minimum.

4. Calculated shell structure

The calculated shell structure reported here (figs. 1 and 6, table 1) is obtained from self-consistent calculations of the electron levels using the background potential of a positively charged jellium sphere [4], whose radius $R=r_{Al}N^{1/3}$, is chosen appropriate to the density of aluminum, $r_{Al}=2.98\ a_0$. In the experiments, the level filling n_e is linked to N and thus to R, so that observed properties are all related to the energy gaps, or the state density, near the Fermi level. Therefore the electronic structure calculation should ideally be repeated for each value of N. However, the self-consistent orbital energies are found to evolve gradually with R and n_e, so that in practice we deduce the level-ordering and gaps from computations carried out only on the filled-shell clusters. Size-variations in the properties of clusters that are not too much smaller than a filled-shell cluster are computed from the energy-level structure of that cluster. In this way, one obtains size-to-size variations in the electronic part of the cohesive energy. The second difference in this quantity, denoted $\Delta_2(E)$ [4], which exhibits a peak at each major shell closing [3], is compared with experimental abundances in fig. 6 to indicate qualitative correspondences and regions of quantitative discrepancy. As pointed out above, this agreement with the experimental results becomes increasingly good at larger sizes.

5. Discussion and conclusions

The pronounced electronic shell structure presented earlier [8] for trivalent clusters is found to continue to quite large clusters, and can best be seen as a periodic modulation, in square root of energy, of the electronic density of states. Comparison of the shell closings found for $n_e=100$–1300 electrons with calculations based on a spherical-jellium background potential show that for Al_N in the range $140<N<250$ atoms, several discrepancies persist, but for $N>250$ atoms, the agreement is excellent. The disagreements are attributed to the symmetry-breaking caused by the ionic lattice, which is neglected in the spherical model. (Generally, such symmetry-breaking effects can take the form of enhanced short-wavelength modulations due to deeper atomic pseudopotentials or boundary conditions introduced by faceting of the cluster surface, but these cannot be separated at this time.) These deviations seem to be smaller for the larger In-atom clusters, at least over the range studied, in agreement with earlier findings on smaller clusters. Similarly, the excellent success reported [14,15] for the spherical model for Na and Cs clusters in the large-size range confirms that they are more jellium-like than Al. The range of sizes studied here was not sufficient to confirm the existence of supershells, as only one super shell minimum is predicted in this range.

This phenomenon of shell structure in large clusters seems to be deserving further study, also from a semi-classical picture [11,13], and particularly in connection with possibly related effects in nanofabricated materials (quantum wires and dots) [19] sharing the same length scale (≈ 2 nm) as the larger clusters examined here. Finally, it seems likely that a photoemission spectrum, obtained for the entire band [20] of a single-sized large aluminum cluster (500 atoms), should be capable of directly exhibiting the density of states oscillations.

Acknowledgement

The authors are indebted to T.P. Martin and K. Hansen for providing prepublication copies of refs. [13] and [12], respectively. Discussions of various points with them and with W.D. Knight, O. Echt, G.S. Ezra and U. Landman are also acknowledged. B. Salisbury assisted in model computations, which benefitted from the advice of M.T. Chou. Funding has been provided by the National Science Foundation and the Office of Naval Research.

References

[1] R. Kubo, J. Phys. Soc. Japan 17 (1962) 975;
L.P. Gor'kov and G.M. Eliashberg, Soviet Phys. JETP 21 (1962) 940.
[2] W.P. Halperin, Rev. Mod. Phys. 58 (1986) 533.
[3] W.D. Knight, K. Clemenger, W.A. Heer, W.A. Saunders, M.Y. Chou and M.L. Cohen, Phys. Rev. Letters 52 (1984) 2141;
W.D. Knight, W.A. de Heer and K. Clemmenger, Solid State Commun. 53 (1985) 445.

[4] W. Ekardt, Phys. Rev. B 29 (1984) 1558; J.L. Martins, R. Car and J. Buttet, Surface Sci. 106 (1981) 265;
W. Ekardt and Z. Penzar, Phys. Rev. B 38 (1988) 4273.
[5] W.A. de Heer, W.D. Knight, M.Y. Chou and M.L. Cohen, Solid State Phys. 40 (1987) 94;
M.L. Cohen, M.Y. Chou, W.D. Knight and W.A. de Heer, J. Phys. Chem. 91 (1987) 3141.
[6] K. Clemenger, Phys. Rev. B 32 (1985) 1395;
T.H. Upton, J. Chem. Phys. 86 (1987) 7054.
[7] N. Malinowski, H. Schaber, T. Bergmann and T.P. Martin, Solid State Commun. 69 (1989) 733.
[8] K.E. Schriver, J.L. Persson, E.C. Honea and R.L. Whetten, Phys. Rev. Letters 64 (1990) 2539.
[9] J.L. Persson, K.E. Schriver, E.C. Honea and R.L. Whetten, Photoionization Spectroscopy of Aluminum and Indium Clusters, to be published.
[10] H.-P. Cheng, R.S. Berry and R.L. Whetten, Phys. Rev. B 43 (1991) 10647.
[11] R. Balian and C. Bloch, Ann. Phys. 69 (1972) 76;
M.V. Berry and M. Tabor, Proc. Roy. Soc. A 349 (1976) 101.
[12] V.M. Strutinskii and A.G. Magner, Soviet J. Part. Nucl. 7 (1976) 138.
[13] H. Nishioka, K. Hansen and B.R. Mottelson, Phys. Rev. B 42 (1990) 9377.
[14] s. Bjørnholm, J. Borggreen, O. Echt, K. Hansen, J. Pedersen and H.D. Rasmussen, Phys. Rev. Letters 65 (1990) 1627.
[15] H. Göhlich, T. Lange, T. Bergmann and T.P. Martin, Phys. Rev. Letters 65 (1990) 748.
[16] T.P. Martin, T. Bergmann, H. Göhlich and T. Lange, Chem. Phys. Letters 172 (1990) 209.
[17] T.P. Martin, T. Bergmann, H. Göhlich and T. Lange, Chem. Phys. Letters 176 (1990) 343.
[18] W.C. Wiley and I.H. McLaren, Rev. Sci. Instr. 26 (1955) 1150.
[19] M.A. Reed and W.P. Kirk, eds. Nanostructure physics and fabrication (Academic Press, New York, 1990).
[20] O. Chesnovsky, K.J. Taylor, J. Conceicao and R.E. Smalley, Phys. Rev. Letters 64 (1990) 1785.